Dual-modal SERS/fluorescence AuNP probe for mitochondrial imaging

Charlotte J. Eling,[a,b] Thomas W. Price,[a] Addison R. L. Marshall,[b] Francesco Narda Viscomi,[b] Peter Robinson,[b] George Firth,[a] Ali M. Adawi,*[b,e] Jean-Sebastien G. Bouillard,*[b,c,e] and Graeme J. Stasiuk*[a,d]
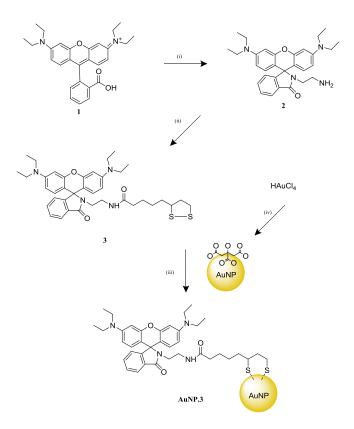
Abstract: A novel SERS/fluorescent multimodal imaging probe for mitochondria has been synthesised using 12 nm diameter gold nanoparticles (AuNP) surface functionalised with a rhodamine thiol derivative ligand. The normal pH dependant acidic fluorescence of the rhodamine based ligand is inversed when conjugated with the AuNP and higher emission intensity is observed at basic pH. This switch correlates to a pKa at pH 6.62, which makes it an ideal candidate for a pH sensitive imaging probe in the biological range (6.5-7.4). The observed pH sensitivity when attached to the AuNP is thought to be due to the formation of a spirolactam ring on the ligand, going from positively charged (+18 mV) to negatively charged (-60 mV) as the pH is changed from acidic to basic. Additionally, conjugation of the ligand to the AuNP serves to enhance the Raman signal of the rhodamine ligand through Surface Enhanced Raman Scattering (SERS). Confocal microscopy has shown that the probe enters HEK293 (kidney), A2780 (ovarian cancer) and Min6 (pancreatic beta) cells within an hour and a half incubation time. The probe was shown to localise in the mitochondria, thus providing a novel pH dependent SERS/fluorescent multimodal imaging probe for mitochondria.

Introduction

Molecular imaging is the visualization of the body beyond the cellular to the sub-cellular scale. This is where the most interesting diagnostic targets for disease are found, and are present at low concentrations, typically in the nano- or pico-molar range. Molecular imaging has only been possible due to the advances in molecular biology and genetics over the past twenty years. [1] Molecular imaging utilizes a wide range of diagnostic modalities in the clinic, such as magnetic resonance (MR) imaging, sing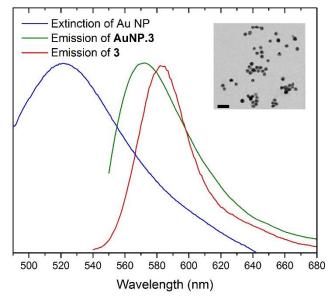le photon emission computed tomography (SPECT), positron emission tomography (PET), ultrasound and optical imaging (OI). [2] However they all suffer draw backs, for instance MR has excellent anatomical resolution; but suffers at the molecular scale due to its intrinsic low sensitivity. In order to overcome the inherent problems of individual modalities, multimodal contrast agents is an area of research that shows great promise. This is the combination of two or more of these modalities to allow for visualization of cellular function and structure in a non-invasive manner. [3]

Scheme 1. Synthesis of dual modal fluorescent/Raman probe **AuNP.3**. (i) Diethyl amine, (ii) Lipoic acid, EDC, DMAP, (iii) Methanol, TCEP, NaOH, (iv) H2O, sodium citrate.

In parallel, gold nanoparticles (AuNP) have been successfully used in medical applications as nanocarrirers for imaging agents, [4] drug delivery and targeted therapy.[5] This is due to the reproducible synthesis of specific sizes AuNPs,[6] facile loading techniques through surface chemistry [7] and gold's biocompatibility compared to other nanoparticles. As AuNPs do not suffer from oxidation effects as quickly as other metallic nanoparticles, they can be used for a variety of applications. [7] There has been increasing interest in cancer detection and

[a]   C. J. Eling, T. W. Price, G.Firth and Dr G. J. Stasiuk
        School of Life Sciences, Biomedical Section,
        University of Hull,
        Cottingham road, HU6 7RX, UK
        E-mail: g.stasiuk@hull.ac.uk
[b]   C. J. Eling, A. R. L. Marshall, F. Narda Viscomi, Dr A. Adawi, and Dr J-S. G. Bouillard
        School of Mathematics and Physical Sciences, Department of Physics and Mathematics,
        University of Hull,
        Cottingham road, HU6 7RX, UK
[c]   Dr J-S. G. Bouillard
        Department of Physics,
        King's College London,
        Strand, London, WC2R 2LS
[d]   Dr G. J. Stasiuk
        Positron Emission Tomography Research Centre,
        University of Hull,
        Cottingham road, HU6 7RX, UK
[e]   Dr A. Adawi, and Dr J-S. G. Bouillard
        G. W. Gray Centre for Advanced Materials
        University of Hull,
        Cottingham road, HU6 7RX, UK

        Supporting information for this article is given via a link at the end of

therapy, where AuNPs have been used as hyperthermia therapy agents.[5]

Figure 1. Emission spectra of **3** and **AuNP.3**, (H2O, 298K), extinction of the

AuNP, inset TEM of **AuNP.3** scale bar 40 nm.

Additionally, the Localised Surface Plasmon Resonance (LSPR), associated with AuNPs can be tuned by engineering the size and shape of the nanoparticle. [8] The strong field confinement and enhancement linked to the LSPR can be used to enhance Raman signals of nearby molecules, including conjugated aromatic attached to metallic nanoparticles, resulting in Surface Enhanced Raman Scattering (SERS), an ultrasensitive vibrational spectroscopic technique. [8] In recent years, SERS has been used as an imaging tool for several molecular events. [9] This enhancement in Raman signal has recently been applied to medical imaging and presents a novel modality as a diagnostic tool. [9] In combination with optical imaging, SERS can provide a useful tool to obtain information on the local chemical environment *in vivo*. [10] As a result, SERS probes have been used as nano sensors for cellular functions including pH, and biomarker localisation. [9] These probes use organic fluorophores such as Rhodamine 6G in conjunction with AuNPs to obtain enhanced Raman signal, and are coupled to antibodies for localizing cancer markers such as PLCγ1. [11] Rhodamine derivatives have received significant attention as fluorescent sensors due to their visible absorption and emission wavelengths, large absorption coefficients, and high quantum yields. [12] They have been used in a wide range of applications, having great success as chemosensors (both *in vitro* and *in vivo*),[13,14] and dual-modal imaging agents.[15,16,10] Mitochondria present excellent targets for molecular imaging of cancer, It is known that the mitochondrial potential in cancer cells is greater than that of healthy cells,[17] and the design of a probe that can accumulate in these energized mitochondria will lead to a tumor-targeting agent. In recent years derivatives of rhodamine have been successfully shown to localise with the mitochondria of tumour cells, [18-20] as their

cationic form localises as a result of the increased negative mitochondrial potential.[21-23] Under acidic conditions, the rhodamine moiety exists in its highly fluorescent pink-coloured form. As the pH increases the structure converts to form a spirocyclic ring, which is colourless and non-fluorescent. This ring-formation mechanism of rhodamine has also led to its extensive use as a pH-sensitive probe as well as chemosensor for metal detection. [24-26]. Herein we show the first multimodal SERS/fluorescent probe based on AuNPs and thiol rhodamine derivative that localises within mitochondria.

Results and discussion

We present a AuNP-Rhodamine conjugate exhibiting Raman enhancement and pH dependent fluorescence, which shows localisation within the mitochondria of cells. The dual modal probe **AuNP.3** was formed in four steps: the synthesis of the AuNP and rhodamine thiol ligand followed by surface functionalisation (Scheme 1). The monodisperse AuNPs were synthesised using the Turkevich method [27, 28] to yield citrate coated AuNPs of diameter 12 nm ± 1.5 nm, determined by TEM (Figure S20). It was found that the plasmonic resonance of the citrate capped AuNPs peaks at a wavelength of 521 nm (Figure 1). The second component of **AuNP.3** is the rhodamine thiol derivative, which was synthesised in a two-step method. The first step is the addition of an amino functionalisation for coupling to the lipoic acid. This amino functionalisation was undertaken on the phenyl carboxylate of **1**, through the means of an amide bond formation with ethylenediamine, resulting in product **2** with a yield of 84%. The second step involved the addition of a lipoic acid through the formation of an amide bond to give compound **3** with a yield of 29%, under standard coupling condition with the carbodiimide N-Ethyl-N'-(3-dimethylaminopropyl)carbodiimide, and 4-Dimethylaminopyridine as the base. The dithiol on the lipoic acid allowed the molecule to attach to the nanoparticle through two strong Au-S bond. It should be noted that the addition of the lipoic acid reduced the solubility of **3** in water. The photophysical properties of **3** were found to be similar to the standard rhodamine derivatives with an emission maxima at a wavelength of 582 nm when excited at the maximum absorption peak of 565 nm (Figure 1). The small Stokes shift of ~ 20 nm, is expected as the fluorescence of rhodamine which has been extensively studied. [29] Ligand exchange was undertaken in a 1:1 mixture of methanol water with a pH range of 7-8 to replace the citrate coating of the AuNPs with **3**. Tris(2-carboxyethyl)phosphine) (TCEP) was added to reduce the dithiol bond, keeping the pH high enough as not to protonate the free thiols of **3**, allowing for functionalisation to the surface of the AuNP to produce **AuNP.3**. This ligand exchange method had already been successfully used with lipoic acid Gd(III) chelate derivatives on quantum dots. [30,31] Thermogravimetric analysis (TGA) of **AuNP.3** shows that there are approximately 2264 ligands on the surface of each AuNP. This was confirmed by absorption spectra which yielded a result of 2398 ligands per nanoparticle (Figure S17). Infrared (IR)

absorption spectroscopy confirms the presence of **3** on the surface of the product **AuNP.3**,

to a quantum yield of 0.8% at a pH of 8.1, and 0.2% at pH 5.1. The inverse pH response also shows a shift of the pKa from 4.59
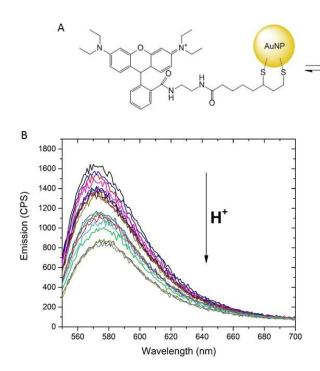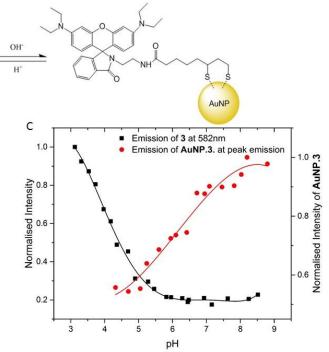

Figure 2. (A) pH-mediated ring opening of the intramolecular spirirolactam of **AuNP.3**, yielding a highly fluorescent species. (B) pH-dependent emission spectra of **AuNP.3** (λex = 535 nm, λem = 570 nm); (C) pH titration curve used to determine pKa of **3** and **AuNP.3**.

(Figure S22). The rhodamine functionalised AuNP **AuNP.3** acts as a multimodal SERS/fluorescence imaging probe with pH sensitivity. The optical properties of both **3** and **AuNP.3** were investigated at various pHs. It was found that the emission intensity of **3** increased in more acidic conditions. As the pH is lowered the spirolactam ring of the molecule opens, yielding a greater fluorescence (Figure S23), as observed in other rhodamine conjugates. [10,32] Correspondingly, the quantum yield of **3** at pH 7.5 was found to be 16.6% while at pH 4.3 it was 25.9%. A titration curve was produced by plotting the emission maxima of **3** at 582nm as a function of pH, yielding a pKa value of 4.59, which is comparable to that of rhodamine DOTA conjugates with pKa of 5.5. [10,32] However in the case of **AuNP.3** the opposite effect is observed with a higher fluorescence emission observed at high pH rather than low pH, corresponding

to 6.62 (Figure 2c) on the AuNP. This pKa is ideal for responsive imaging in biological applications (pH range from 6.5-7.4). This switch in pH sensitivity could be due to the change in localized charge about the AuNP, reflected in the zeta potential of **AuNP.3** which ranges from +18 mV at pH 5.2 to -60 mV at pH 7.8. This change in charge occurs when the spirolactam ring opens upon protonation at low pH (Figure S19) making it more positive. Additionally, the emission maximum of **AuNP.3** was shifted to a wavelength of 570 nm in comparison to 582 nm for **3**. This blue-shift in emission after speciation is due to the change in the photonic environment around the ligand as a result of binding to the surface of gold (Figure 1/S24). Sun *et. al.* have shown that conjugation of pH insensitive dyes such as TAMRA to ultra-small AuNPs can enhance the pH sensitivity fluorescence properties of the dyes, but also broaden the pH range of fluorescein, suggesting changes in local surface charges after dye dimerization for this. [33]

The lifetime of **3** shows two distinct components, representing two different decay rates. At low pH (3.82), and higher quantum yield, there is a slow component with a lifetime of 2.44 ns having a weighting of 63%, with the remaining 37% corresponding to the fast component of 0.58 ns. However as the pH is increased (6.26) and the quantum yield decreases, the lactam ring is formed and the weighting of each channel is reversed as 31% now corresponds to a fluorescence lifetime of 2.37 ns and 69% to a lifetime of 0.34 ns. This change in lifetime along with the evolution of the quantum yield with pH clearly illustrates the increase of a non-radiative decay channel with protonation of the ligand.

The lifetime of **3** was also measured in a series of solvents (Table S1) including ethanol where it was found that 93% of the fluorescence corresponds to a lifetime of 1.34 ns with the

Table 1. Lifetime of **AuNP.3** at high and low pH at 530nm and 570nm.

		530 nm		575 nm	
pH 4.31	Lifetime (ps)	<100	1700	611	2200
	Weighting	92 %	8%	31%	69%
pH 8.16	Lifetime (ps)	<100	1400	657	2800
	Weighting	85%	15%	42%	58%

remaining corresponding to a lifetime of 2.13 ns, which is in agreement to reported values for rhodamine B. The observed change of the fluorescence lifetimes with the solvent, indicates solvent quenching effects on **3**, particularly in water (Table S1).

Due to the emission shift of **AuNP.3**, and in order to quantify the coupling to the plasmonic resonance, the lifetime of **AuNP.3** was measured at emission wavelengths 530 nm (corresponding to a full overlap with the LSPR of the AuNP) and 575 nm (corresponding to the tail of the LSPR) (Table 1). Both at low and high pH, the lifetime is reduced from ~600 ps away from the plasmonic resonance (575 nm) to below 100 ps (limited by the instrument response) on the plasmonic resonance (530 nm). Along with the decrease in emission intensity, the reduced lifetime of **AuNP.3** around the plasmonic resonance (table 1), shows that the fluorescence is being increasingly quenched by the AuNP as the spectral overlap with the plasmonic resonance increases. This is also consistent with the evolution of the emission spectrum of **AuNP.3**, as the intensity at a wavelength of 530 nm decreases faster with pH compared to a wavelength of 575 nm. Additionally, it can be seen that the weight of the fast component (sub-100 ps) is reduced as the pH is increased, in agreement with the reversed pH curve of **AuNP.3** with respect to **3**.
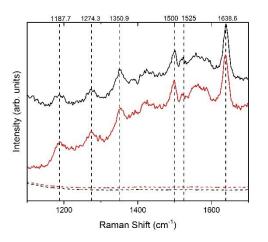

Figure 3. Raman spectra of **3** (dash lines) and **AuNP.3** (solid lines), at low pH (red), and high pH (black).

Raman spectroscopy of **3** and **AuNP.3** deposited on a glass slide (Figure 3) shows clear enhancement of the characteristic rhodamine Raman scattering signals, such as the aromatic C–C bending and C-C stretching at 1638 cm^{-1} and the Aromatic C–H bending at 1500 cm^{-1}, [34] when attached to the AuNP surface **AuNP.3** compared to the control sample prepared from the ligands on their own, **3**, indicating that **AuNP.3** has the potential to work as dual modal SERS/fluorescence probe.

Thus far we have shown that **AuNP.3** give both pH dependent emission *via* fluorescence with the switch occurring at a pH of 6.62 and enhanced Raman signal. To show that it can be used as an imaging tool **AuNP.3** was incubated with Human Embryonic Kidney (HEK 293) (figure S26-31), Min-6 cells (Figure S37-42) and Ovarian Cancer (A2780) cells (Figure 4, Figure S32-36). This was to primarily show that the nanoconstruct would go inside cells

and that the rhodamine ligand would direct it to the mitochondria to allow for potential cancer imaging. As can be seen in Figure 4, **AuNP.3** enters the cells within 90 minutes and is localised inside the mitochondria. This is confirmed by the use of Mitotracker deep red. There is no co-localisation with the lysotracker blue confirming localization in the mitochondria of all cell lines studied. It is postulated that the charge of the **AuNP.3** is thought to direct the nanoparticle to the mitochondria. This has been seen with the smaller molecule dual modal agents, where charge is important to intracellular localization of the probe. [35] It can be postulated that this entrance is through endocytosis as most of **AuNP.3** appears in vesicular structures and is too big to diffuse through the cell membrane. MTT studies also show **AuNP.3** to be non-toxic at concentrations used for imaging (Figure S25), with IC$_{50}$ in the millimolar range (12 mM [Au]). In comparison to Rhodamine 6G AuNP based probes which have shown internalisation into endothelial cells [36], **AuNP.3** shows localization to the mitochondria in three different cell lines, thus giving a mitochondrial targeted multimodal probe.
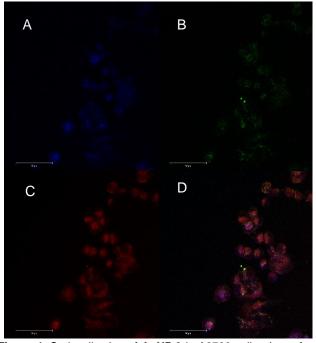

Figure 4. Co-localisation of **AuNP.3** in A2780 cells *via* confocal microscopy. A) Lyso-tracker staining, B) **AuNP.3**, C) Mito-tracker staining and D) overlay. (RPMI 1640 media, 298K)

Conclusions

We describe a dual-modal SERS/fluorescence imaging agent that is pH sensitive, with excellent fluorescent and Raman properties, which may potentially be used to monitor mitochondria in cancer. The dual-modal probes **AuNP.3** show fluorescence changes with a large shift in the emission spectrum, from λ_{em} = 582 nm to λ_{em} = 570 nm upon surface functionalization to AuNPs of 12 nm in diameter. The second advantage that arises from functionalization to the AuNP is an inverse in pH dependent

emission, with high emission observed at basic pH and low signal intensity at acidic pH with a pKa of 6.62. Compared to **3** which has a pKa of 4.59, with high emission seen at acidic pH. **AuNP.3** also show significant Surface Enhanced Raman Scattering (SERS) compared to **3**. When examined in cell lines, (HEK293, Min-6 and A2780) **AuNP.3** showed localization to mitochondria, and relatively poor uptake into other vesicles inside the cells, reflecting excellent cell permeability and localization to the energy centers of the cell. This gives the option to take **AuNP.3** forward as a multimodal SERS/fluorescent probe for mitochondrial imaging, in particularly for cancer, although further validation is required. We therefore believe that **AuNP.3** provides a first stage model for the preparation of probes which may ultimately be of clinical utility.

Experimental Section

Reagents

Rhodamine B, Lipoic acid, 1-Ethyl-3-(3-dimethylaminopropyl)carbodiimide (EDCI), 4-Dimethylaminopyridine (DMAP), HAuCl4 and Trisodium citrate were obtained from Sigma-Aldrich. HPLC water was used throughout and purchased from VWR chemicals.

Apparatus

The Transmission Electron Microscope used was a JEOL 2010 Transmission Electron Microscope at 200kV, the images were taken with a Gatan US4000 camera. FTIR spectra was taken on Perkin Elmer Rx FTIR x2 with diamond ATR, DRIFT attachment. Zeta potential was taken on Malvern, Zetasizer Nano-z5. Cellular imaging was taken on a Zeiss LSM 710 Confocal scanning microscope.

Fluorescence Measurements

All fluorescence measurements were made with a Horiba Fluoromax-4P spectrofluorometer in a 10 mm quartz cuvette. All spectra was taken in either aqueous or ethanolic solutions depending on solubility. Fluorescence quantum yields were obtained using a previous reported method using a reference compound of rhodamine B in ethanol.

The lifetime was measured in a 10 mm quartz cuvette. Exciting at 532 nm for **3** and 485 nm for **AuNP.3**. The emission was collected at 575 nm and 530 nm for both off and on the plasmonic resonance respectively using a Becker and Hickl HPM-100 detector.

pH Titration

A 0.15mM solution of 3 in 0.1M KCl (2ml) was prepared and then added to a 10mm quartz cuvette. The pH was monitored using a digital pH meter (Jenway 3520) with a glass electrode (Mettler Toledo 51343160). The pH was adjusted to 8.5 using 1mM NaOH solution then lowered to acidic conditions by adding small aliquots of 1mM HCl. Fluorescence spectra was taken for a range of pH with a 3nm excitation slit width, 1nm emission slit and 0.5s acquisition time. This was repeated for **AuNP.3** under the same conditions.

Raman

For Raman measurements, the samples were prepared through spin-coating a thin layer of either **3** or **AuNP.3** onto glass substrates at a speed of 500rpm for 30 secs. Raman measurements were taken using a Raman setup equipped with a 532 nm DPSS laser to excite the samples. Raman signal was collected using a 0.55NA, 50x objective lens then directed toward a Horiba i320 spectrometer that coupled to a nitrogen cooled symphony CCD. In all measurements we used a 10 mW excitation power, an acquisition time of 5s and a spectrometer slit width of 0.1mm.

Gold nanoparticle synthesis

Spherical 15nm gold nanoparticles were prepared by citrate reduction of HAuCl$_4$ according to literature [37]. The synthesis is as follows; Gold hydrochlorate (7mg, 0.8nmol) is added into 20mL of an aqueous solution. This is then heated to 75°C in a 3 neck round bottom flask by means of a heating mantle to ensure a homogenous temperature. The liquid is vigorously stirred using a magnetic stirrer. In a separate round bottom flask a further 20mL of aqueous solution is heated with the addition of trisodium citrate (40mg, 7.7mmol). When the gold hydrochlorate solution has come to the boil the preheated trisodium citrate is then added. The solution quickly turns to a wine-red as the nanoparticles increase in size. To prevent aggregation the solution was left to stir for 40mins then span down in a centrifuge at 13300rpm for 20 minutes at a low temperature. As the reaction is temperature dependent this stops the reaction causing the citrate to cap the nanoparticle and avoid the nanoparticles aggregating. It was found after 20 minutes the nanoparticles had reached the maximum size of 15nm. From TEM and extinction spectra the nanoparticles are more spherical and monodisperse after a time of 40 minutes.

Ligand synthesis

NMR was obtained using Oxford A4500 at 400MHz. Mass spectroscopy was obtained using Avion Expression CMS with a Hitachi chromaster 5110 pump.

2 was synthesised as follows. Rhodamine B (4.8g, 10mmol) was dissolved in EtOH (30ml). Ethylenediamine (4.48g, 13mmol) was added dropwise. The reaction mixture was heated to reflux temperatures for 15 hours until it loses its red colour. The solvent was removed in vacuo. Water is then added to the resultant and extracted in Dichloromethane. The compound was washed twice with water and dried over Magnesium sulfate. The solvent was removed again in vacuo yielding compound (1). 1H NMR (400MHz, CDCL3): δ 1.16 (t, 14H, 3JHH = 7.04Hz), 2.40 (t, 2H, 3JHH = 6.53Hz), 3.18 (t, 2H, 3JHH = 6.53Hz), 3.30-3.36 (m, 9H), 6.25-6.28 (m, 2H), 6.37(d, 2H, 3JHH = 2.56Hz), 6.42 (s, 1H), 6.44 (s, 1H), 7.08-7.10 (m, 1H), 7.42-7.46 (m, 2H), 7.88-7.92 (m, 1H). 13C NMR (100MHz, CDCl3): 12.65, 40.94, 43.92, 44.49, 64.96, 97.80, 105.76, 108.17, 122.81, 123.95, 128.07, 128.79, 131.34, 132.48, 148.83, 153.38, 168.73. ESI-HRMS: calcd for C30H37N4O2 485.29, found m/z 485.85.

3 was synthesised as follows. This is achieved by creating a mixture of compound (2) (100mg, 0.222mmol), (45.7mg, 0.222mmol) lipoic acid, 1-Ethyl-3-(3-dimethylaminopropyl)carbodiimide (EDCI) (42.6mg, 0.222mmol) and 4-Dimethylaminopyridine (DMAP) (27.2mg, 0.222mmol) were dissolved in 1:1 ratio of Acetonitrile : Dimethylformamide (DMF) (5ml). This solution was stirred for 18 hours in which a white precipitate formed corresponding to the DMAP salt. The solution was filtered and purified by silica gel chromatography with 1-5% MeOH/DCM. 1H NMR (400MHz, CDCl3): δ 1.17 (t, 12H, NCH2CH3, 3JHH = 7.14Hz), 1.37-1.47 (m, 2H), 1.58-1.71 (m, 4H), 1.85-1.93 (m, 1H), 2.09 (t, 2H, COCH2CH2R, 3JHH = 7.51Hz), 2.40-2.47 (m, 1H), 3.03-3.19 (m, 4H), 3.28-3.36 (m, 10H), 3.51-3.58 (m, 1H), 6.26-6.29 (m, 2H), 6.37 (d, 2H, 3JHH = 2.38Hz), 6.41-6.44 (m, 2H), 6.88-6.9 (m, 1H), 7.07-7.09 (m, 1H), 7.45-7.47 (m, 2H), 7.89-7.91 (m, 1H), 8.02 (s, 1H). 13C NMR (100MHz, CDCl3): 12.77, 25.45, 29.04, 34.94, 36.52, 38.54, 40.27, 40.84, 44.44, 56.53, 65.74, 97.84,

104.75, 108.35, 122.89, 124.04, 128.50, 130.52, 132.96, 148.94, 153.40, 153.98, 170.10, 172.69. ESI-HRMS: calcd for C38H49N4O3S2 673.32, found m/z 673.52.

Ligand Exchange

The AuNPs surfaces were modified to obtain **AuNP.3**. The rhodamine thiol was bound to the nanoparticle surface by Au-S bonding. This was obtained by mixing together Au Np (2.5mg, 0.18nmol), RhB thiol (1.18mg, 1.8umol) and TCEP (5.03mg, 18umol). A solution of methanol (0.5ml) and HPLC water (3.5ml) was added and the pH adjusted between 7 and 8. The solution was then left to stir overnight at room temperature. The resultant was then span down at 6000rpm for 2 minutes and repeated until the suspension was clear, resuspended in water and sonicated. The fluorescence spectra was obtained at room temperature exciting at 535nm which is the maximum excitation for the probe and at 565nm, the maximum excitation for the ligand. The low emission was evidence that the RhB molecule had attached to the nanoparticle surface and was being quenched by the Au. The spectra was also evidence that no excess rhodamine was in the sample.

In Vitro studies

The A2780, Min6 and HEK cells were washed and resuspended in RPMI 1640 and DMEM respectively. The cells were then loaded into Starstedt lumox dish 35 and left to grow overnight in 2ml of RPMI 1640 and DMEM. They were then washed twice with PBS and then incubated with RPMI 1640 medium or DMEM, 100μl of the nanoparticles suspended in water at a concentration of 5.4×10^{13} nanoparticles per ml, 4μl of lysotracker, mitotracker and DAPI. After an hour and half all media and dyes were removed. The cells were then washed with PBS and PFT was added to fix the cells. After ten minutes incubation at room temperature, the PFT was removed and the cells washed again with PBS and stored in PBS at 4 degrees. They were imaged using a Zeiss LSM 710 Confocal scanning microscope.

MTT Assay

To determine cell viability the MTT metabolic assay was used. A2780 cells were cultured in a 96-well plate at 37°C for 24 hours and then exposed to varying concentrations of **AuNP.3** for a further 24 hours. Due to the small overlap in absorbance a control was ran of just media and nanoparticles to eliminate any absorbance from the nanoparticles. A solution of MTT (5 mg ml^{-1} in PBS) was added to each well and left to incubate for a further 4 hours. All the media was then removed and the plates washed with PBS. The resultant formazan crystals were dissolved in Dimethyl sulfoxide and the absorbance measured at 570nm and 690 nm.
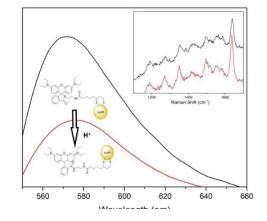
Acknowledgements

Keywords: Gold nanoparticle • Rhodamine• cellular imaging • optical imaging • Raman

[1]   M. Doubrovin, I. Serganova, P. Mayer-Kuckuk, V. Ponomarev and R. G. Blasberg, *Bioconjugate. Chem.,* **2004**, 15, 1376-1388.
[2]   K. M. Brindle, *Br. J. radiol.* **2003**, 76, S111-S117.
[3]   L. E. Jennings and N. J. Long. *Chem. Commun.*, **2009**, 3511-3524
[4]   S.Sung, H. Holmes, L. Wainwright, A. Toscani, G.J. Stasiuk, A. White, J. Bell, J. Wilton-Ely, *Inorganic Chem.*, **2014**, 53, 1989–2005
[5]   T. Stuchinskaya, M. Moreno, M. J. Cook, D. R. Edwards, D. A. Russell, *Photochem. Photobiol. Sci.*, **2011**. 10, 822-831.
[6]   S. K. Ghosh and T. Pal, *Chem. Rev.* **2007**, 107, 4797−4862
[7]   K. Saha, S. S. Agasti, C. Kim, X. Li, and V. M. Rotello, *Chem.Rev.* **2012**, 112, 2739−2779.
[8]   K. M. Mayer and J. H. Hafner, *Chem. Rev.*, **2011**, 111, 3828–3857
[9]   Y. Wang, B. Yan and L. Chen, *Chem. Rev.* **2013**, 113, 1391−1428
[10]   C. Rivas, G. J. Stasiuk, J. Gallo, F. Minuzzi, G. A. Rutter, N. J. Long, *Inorganic Chem.,* **2013**, 52, 14284–14293.
[11]   S. Lee, S. Kim, J. Choo, S. Y. Shin, Y. H. Lee, H. Y. Choi, S. Ha, K. Kang and C. H. Oh, *Anal. Chem.,* **2007**, 79, 916–922.
[12]   M. S. T. Gonçalves, *Chem. Rev.* **2009**, 109, 190−212.
[13]   L. Yuan, W. Lin, K. Zheng, L. He, W. Huang, *Chem. Soc. Rev.* **2013**, 42, 622−661.
[14]   C. Suksai, T. Tuntulani, *Chem. Soc. Rev.* **2003**, 32, 192−202.
[15]   Y. Zhou, Y.-S. Kim, X. Yan, O. Jacobson, X. Chen, S. Liu, *Mol. Pharmaceutics.* **2011**, 8, 1198−1209.
[16]   Y. You, E. Tomat, K. Hwang, T. Atanasijevic, W. Nam, A. P. Jasanoff, S. J. Lippard, *Chem. Commun.* **2010**, 46, 4139−4141.
[17]   M. R. Duchen, *Mol. Aspects Med.*, **2004**, 25, 365−451.
[18]   R. C., Jr.; Scadutro, L. W. Grotyohann, *Biophys. J.* **1999**, 76, 469−477.
[98]   M. R. Longmuir, M. Ogawa, Y. Hana, N. Kosaka, C. A. S. Regino, P. L. Choyke, H. Kobayashi, *Bioconjugate Chem.* **2008**, 19,1735−1742.
[20]   L. D. Lavis, T.-Y. Chao, R. T. Raines, *ACS Chem. Biol.* **2006**, 1, 252−260.
[21]   P. D. Hockings, P. J. Rogers, *Biochim. Biophys. Acta*, **1996**, 1282, 101−106
[22]   S. G. Huang, *J. Biomol. Screening,* **2002**, 7, 383−389.
[23]   C. Lefevre, H. C. Kang, R. P. Haugland, N. Malakzadeh, S. Arttamangkul, R. P. Haugland, *Bioconjugate Chem.* **1996**, 7, 482−489.
[24]   X. Chen, T. Pradhan, F. Wang, J. S. Kim, Yoon, *J. Chem. Rev.*, **2012**, 112, 1910−1956.
[25]   Q. A. Best, R. Xu, M. E. McCarroll, L. Wang, D. J. Dyer, *Org. Lett.*, **2010**, 12, 3219−3221.
[26]   M. H. Lee, J. H. Han, J. H. Lee, N. Park, R. Kumar, C. Kang, J. S. Kim, *Angew. Chem., Int. Ed.*, **2013**, 52, 6206−6209.
[27]   B.V. Enüstün, and J. Turkevich, *J. Am. Chem. Soc.,* **1963**. 85, 3317-3328.
[28]   J., Kimling, M. Maier , B. Okenve , V. Kotaidis , H. Ballot , and A. Plech, *J. Phys. Chem. B*, **2006**. 110. 15700-15707.
[29]   M. Beija, C. A. M. Afonso and J. M. G. Martinho, *Chem. Soc. Rev.*, **2009**. 38, 2410-2433.
[30]   G. J. Stasiuk, S. Tamang, D. Imbert, C. Poillot, M. Giardiello, C.Tisseyre, E. L. Barbier, P.H. Fries, M. de Waard, P. Reiss, and M. Mazzanti, *ASC Nano,* **2011**, 5, 8193–8201.
[31]   G. J. Stasiuk, S. Tamang, D. Imbert,, C. Gateau, P.H. Fries, P. Reiss, and M. Mazzanti, *Daltons Trans.,* **2013**, 42, 8197-8200.
[32]   C. Rivas, G.J. Stasiuk, M. Sae-Heng, N.J. Long, *Dalton Trans.*, **2015**, 44, 4976-4985.
[33]   S. Sun, X. Ning, G. Zhang, Y.-C. Wang, C. Peng, and J. Zheng, *Angew. Chem. Int. Ed.* **2016**, 55, 2421 –2424
[34]   S. Lin, Hasi W.-L.-J., Lin X., S.-q.-g.-w. Han, X.-T. Lou, F. Yang, D.-Y. Lin and Z.-W. Lu, *Anal. Methods,* **2015**, 7, 5289-5294.
[35]   J. Pan, B. I. Harriss, C.-F. Chan, L. Jiang, T.-H. Tsoi, N. J. Long, W.-T. Wong, W.-K. Wong, and K.-L. Wong, *Inorg. Chem.,* **2016**, 55, 6839–6841.
[36]   A. Jaworska, T. Wojcik, K. Malek, U. Kwolek, M. Kepczynski, A. A. Ansar, S. Chlopicki and M. Baranska, *Microchim Acta*, **2015**, 182, 119–127.
[37]   G. Frens, *Nat. Phys. Sci*, **1973**. 241, 20-22.

Entry for the Table of Contents

COMMUNICATION

A novel SERS/fluorescent multimodal imaging probe for mitochondria has been synthesised, an AuNP functionalised with a thiol rhodamine derivative. The normal pH dependant fluorescence of rhodamine is inversed with higher emission observed at high pH, with a pKa at pH 6.62. The probe was shown to localise in the mitochondria.

Charlotte J. Eling, Thomas W. Price, Addison R. L. Marshall, Francesco Narda Viscomi, Peter Robinson, George Firth, Dr Ali M. Adawi,* Dr Jean-Sebastien G. Bouillard,* and Dr Graeme J. Stasiuk*